Research Article

Facile Synthesis of Cu Nanocrystals with Morphology Evolution from Transitional Truncated Octahedra to Octahedra

Kuan-Ting Chen, Wei-Chung Chang, Shu-Chen Lu, Po-Yuan Yang, and Hsing-Yu Tuan ⓘD

Department of Chemical Engineering, National Tsing Hua University, Hsinchu, Taiwan 300

Correspondence should be addressed to Hsing-Yu Tuan; gotoam0204@gmail.com

Growth of Cu polyhedral structures with well-defined and controllable shapes faced tremendous synthetic challenges in colloid nanocrystal synthesis in the past few decades. In this article, we report a facile approach for the synthesis of Cu nanocrystals with systematic morphological evolution. Transitional truncated octahedral, edge- and corner-truncated octahedral, all-corner-truncated octahedral, and octahedral structures were obtained in a solution-based reduction reaction by precise tuning reaction time. Four distinct morphologies of nanocrystals have been characterized by SEM technique. The optical properties of these various morphologies of nanocrystals were also investigated, and it indicates that the SPR band shifts red while the shape of nanoparticles evolves from transitional truncated octahedral to octahedral, whose resonant bands are transferred from 590 nm to 620 nm.

1. Introduction

Nanomaterials have aroused significant attention over the past decades due to their unique physical and chemical properties and technical applications. At nanoscale, the physical and chemical properties of crystals are highly related to their size and shape [1–4]. In addition, the activity of nanoparticles also extremely depends on the crystallographic planes which are exposed on the surface of the particles and can be altered by controlling their shapes. Consequently, rational shape-controlled synthesis of metal nanoparticles is a crucial issue to understand their shape-dependent properties and growth mechanism. In previous reports, most efforts have been devoted to the synthesis of nanoparticles which are bounded by low-index {111} and {100} facets. For example, tetrahedral [5], octahedral [6, 7], decahedral [8, 9], and icosahedral [9, 10] nanoparticles are enclosed by {111} facets, and cubic [11, 12] nanoparticles are enclosed by {100} facets. Besides, nanoplates [13, 14] and cuboctahedral [2, 15, 16] nanoparticles are enclosed by both {111} and {100}

facets. It is well known that the surface energies of nano-particles with different crystalline planes are in the order of $\gamma\{110\} > \gamma\{100\} > \gamma\{111\}$, and the evolution of these nanocrystals can be explained by the consequence of minimizing surface energy.

To date, nanoparticles bounded by {110} facets such as rhombic dodecahedron or truncated octahedron have been rarely found. Because the {110} facet has the highest surface energy among low-index facets, it grows faster than {111} and {100} facets, leading to their disappearance during the crystal growth. The synthesis of metal nanoparticles enclosed by high-energy facets is an important but also difficult task because these high-energy facets can exhibit higher activity, thus improving their potential applications in catalysis. Jeong et al. had concentrated their efforts on the preparation of polyhedral Au nanocrystals which are bounded by {110} surfaces [17]. Huang et al. also tried to control different shapes of Cu_2O from cubes to rhombic dodecahedra by adjusting the amount of $NH_2OH\bullet HCl$ [18]. Xiong and Xia have synthesized various shapes of Pd nanocrystals by controlling the crystalline seeds and the growth rates of different

crystalline facets [19]. Various morphologies of noble metal nanoparticles with well-controllable shapes such as Au and Pd have been proposed.

Cu is fully abundant and less costly compared to other noble metals like Au, Ag, Pd, and Pt. It exhibits the second highest electrical conductivity among the metals, ranking only behind Ag. In addition to Au and Ag, Cu nanocrystals are also known to exhibit localized surface plasmon resonance (LSPR) in the visible region [20]. Because of its unique physical and chemical properties, Cu is one of the most important metals in industry. Cu nanoparticles have widespread applications in catalysis including coupling reaction [21], water-gas shift [22, 23], and gas detoxification reaction [24, 25]. The fundamental properties and applications mentioned above contribute to obtain well-defined and controllable morphologies of Cu nanocrystals. However, due to the tendency of the surface oxidation of Cu and the difficulty of reducing cupric ion into zerovalent atoms during the synthesis, the system of synthesized Cu nanocrystals with well-defined shapes is still a big challenge now. Tanori and Pileni had synthesized Cu nanocrystals with different shapes by mixing reverse micelles with excess reducing agents and tried to understand their growth mechanism [26]. Pastoriza-Santos et al. prepared single-crystalline Cu nanoplates by using hydrazine as a reducing agent to reduce copper salt with polyvinylpyrrolidone as a stabilizer [20]. Ko et al. obtained Cu nanoparticles with pyramidal shapes on a gold substrate [27]. Mott et al. also tried their best to control the shape and size of Cu nanocrystals by controlling the reaction temperature and using amine as a capping agent [28]. Guo et al. have developed a facile synthesis of monodisperse Cu nanoparticles and nanocubes in a hydrophobic solution [29, 30]. Recently, our group had concentrated great efforts on Cu nanocubes and nanoctahedrons whose surfaces are entirely enclosed by {100} and {111} facets, respectively. Monodisperse Cu nanocubes with an average edge length of 75.7 nm were obtained by a hot-injection method with trioctylphosphine and octadecylamine as capping agents [12], and Cu nanoctahedrons were also prepared with a similar approach [31]. Recently, various shapes, including bipyramidal, pentatwinned, nanooctahedra, and faceted Cu particles, were also reported [32–35].

Herein, a simple solution-phase approach has been successfully developed for the synthesis of Cu nanoparticles with a series of morphologies. This approach is based on the reduction of CuCl with trioctylphosphine in an oleylamine system. Transitional truncated octahedron, edge- and corner-truncated octahedron, all-corner-truncated octahedron, and octahedron can be obtained with different reaction times. These nanoparticles can be readily prepared without the use of any seeds or extra metal ions, but with oleylamine and trioctylphosphine as ligands only.

2. Experimental Section

2.1. Chemical.
All chemicals were used as received without extra purification. Copper(I) chloride (99.99%) and trioctylphosphine (TOP, 90%) were purchased from Alfa Aesar.

Oleylamine (OLA, 70%) and anhydrous toluene were purchased from Sigma-Aldrich.

2.2. Synthesis of Cu Nanocrystals.
In a typical synthesis of Cu nanoparticles, 0.2 mmol CuCl and 2 ml TOP were added into a vial and preheated at 200°C for 2 hours in a glove box. 18 ml oleylamine (OLA) was added into a three-necked flask and kept under a flow of high-purity argon gas for 30~60 minutes with strong magnetic stirring. The synthesis has to be executed under the protection of inert gas to avoid the oxidation of the Cu nanoparticles by O_2 in the air. After the purge process is finished, OLA is then heated from room temperature to 335°C before the injection of a precursor solution. In order to realize the morphology change of the Cu nanoparticles during the reaction, the reactions were quenched by a water bath at 5 minutes, 10 minutes, 15 minutes, and 20 minutes after injecting the precursor solution. During the reaction, the colour of the solution changed from bright yellow to red-brown, showing the formation of the Cu0 species. The resultant products were purified by centrifugation and washing with toluene to remove excess reagents.

2.3. Characterization.
Transmission electron microscopy (TEM) was obtained by a Hitachi H-7100 electron microscope with an accelerating voltage of 75 kV. High-resolution TEM (HRTEM) and selected area electron diffraction (SAED) images were obtained by a JEOL JEM 2100F electron microscope with an accelerating voltage of 200 kV. Scanning electron microscopy (SEM) images were taken by Hitachi SU4800 field-emission SEM operating at an accelerating voltage of 10 kV. X-ray diffraction (XRD) measurement was measured by a Rigaku Ultima IV X-ray diffractometer using Cu Kα radiation. UV-visible spectrum was measured by a Hitachi U-4100 spectrophotometer at an ambient environment.

3. Result and Discussion

The transitional truncated octahedral, edge- and corner-truncated octahedral, all-corner-truncated octahedral, and octahedral Cu nanoparticles were synthesized by a facile colloid hot solvent synthesis as described in the Experimental Section and in the supporting information. A reaction carried out at 335°C can produce relatively large sizes of nanoparticle forms, and associated with TOP and OLA's interaction with particle surfaces, Cu particles with well-defined surface can be obtained. Figures 1 and 2 show SEM images of the shape evolution of Cu nanoparticles. When the reaction is stopped after reacting for 5 minutes, the product is bounded by a mix of {111}, {110}, and {100} facets with an edge length of about 120 nm, named transitional truncated octahedron. Each particle is enclosed by eight {111} faces, twelve {110} faces, and six {100} faces (as shown in Figure 1). When the reaction time increases to 10 minutes, the shape of the product becomes a similar octahedral form, but the edges and corners of nanoparticles are all truncated. The products are called an edge- and corner-truncated octahedron whose faces are mainly dominated by {111} facets (as shown in Figure 2(a)). When the reaction time further goes to 15
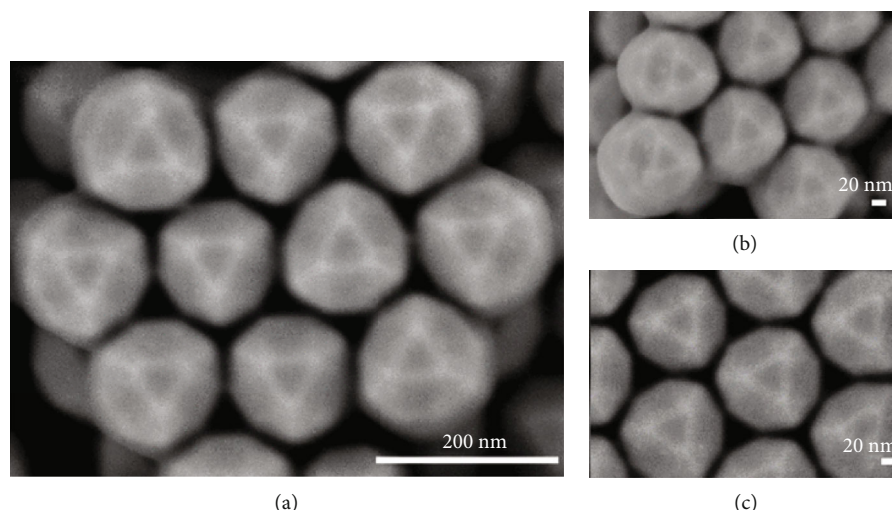
(a)

(b)

(c)

FIGURE 1: SEM images of a transitional truncated octahedron with a reaction time of 5 minutes.

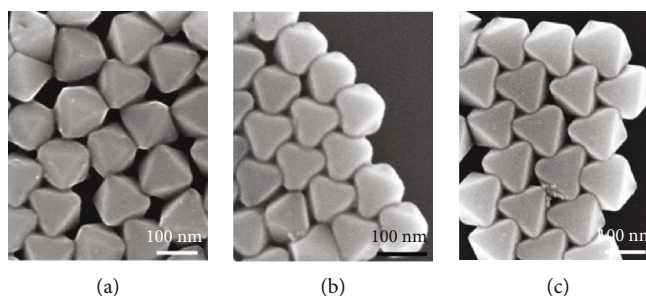

(a)   (b)   (c)

FIGURE 2: SEM images of the shape evolution of Cu nanoparticles with different reaction times: (a) 10 minutes, (b) 15 minutes, and (c) 20 minutes.

minutes, the typical shape of the product transforms into an all-corner-truncated octahedron with the complete growth in the direction of {110}. It has a total of 14 faces, which include 8 {111} facets and 6 {100} facets (as shown in Figure 2(b)). As the reaction reaches 20 minutes, the product becomes an octahedron which is exclusively enclosed by {111} facets (as shown in Figure 2(c)). It is the first time for discovering the shape evolution of Cu nanoparticles enclosed by low-index facets. Although there are few nanoparticles which are a little overacted at each stage in the SEM images, most of them are nearly the same structures. The detailed crystal structures of these Cu nanocrystals were analyzed by high-resolution transmission electron microscopy (HRTEM) and XRD characterization. Figure 3 displays the high-magnification TEM images, the corresponding SAED patterns, and the representative SEM images of individual Cu nanoparticles of various morphologies. The SAED patterns of the transitional truncated octahedral (as shown in Figure 3(a) 2), all-corner-truncated octahedral (as shown in Figure 3(c) 2), and octahedral (as shown in Figure 3(d) 2) Cu nanoparticles are all viewed along the $(02\bar{2})$ direction, except for the edge- and corner-truncated octahedral Cu nanoparticles (as shown in Figure 3(b) 2) with zone axis of [112]. These results indicate that the as-prepared Cu nanoparticles are all single-crystalline and bound by low-index facets. Figure 4 shows the XRD patterns of different morphologies of Cu nanocrystals. The pattern shows the expected refractive peaks of (111), (100), and (110) and confirms that these nanocrystals are face-centered cubic structures. Although these patterns look similar because of the random orientations of nanocrystals on substrates, it shows that the ratio of the intensity of the (111) peak to (200) peak increases from transitional truncated-octahedral to octahedral as nanocrystals with more {111} faces are formed. This trend is expected to consider the growing fractions of {111} faces.

Metal nanoparticles with well-controllable shapes show different optical properties due to the surface plasmon resonance (SPR). The resonance frequency of the oscillation has a strong relationship with a particle's shape [36]. When the shape of a nanocrystal changes, it gives rise to a change in the electric field density at the particle's surface and generates different optical properties. Hence, we study the shape-dependent optical properties of Cu nanoparticles here. In order to investigate the change in optical properties of the shape evolution of Cu nanoparticles, we recorded the spectra by UV-visible spectroscopy. Figure 5 displays a comparison of the absorption spectra with various morphologies of Cu nanoparticles. The spectra of the transitional truncated octahedron and edge- and corner-truncated octahedron show

(A1)

20 nm

(A2)

(111)

(311)

(200)

Zone axis [0$\bar{2}$2]

(A3)

50 nm

(a)

(B1)

20 nm

(B2)

(331)

(220)

(222)

Zone axis [112]

(B3)

50 nm

(b)

(C1)

100 nm

(C2)

(200)

(111)

Zone axis [0$\bar{2}$2]

5 1/nm

(C3)

50 nm

(c)

(D1)

100 nm

(D2)

(220)

(200)

(111)

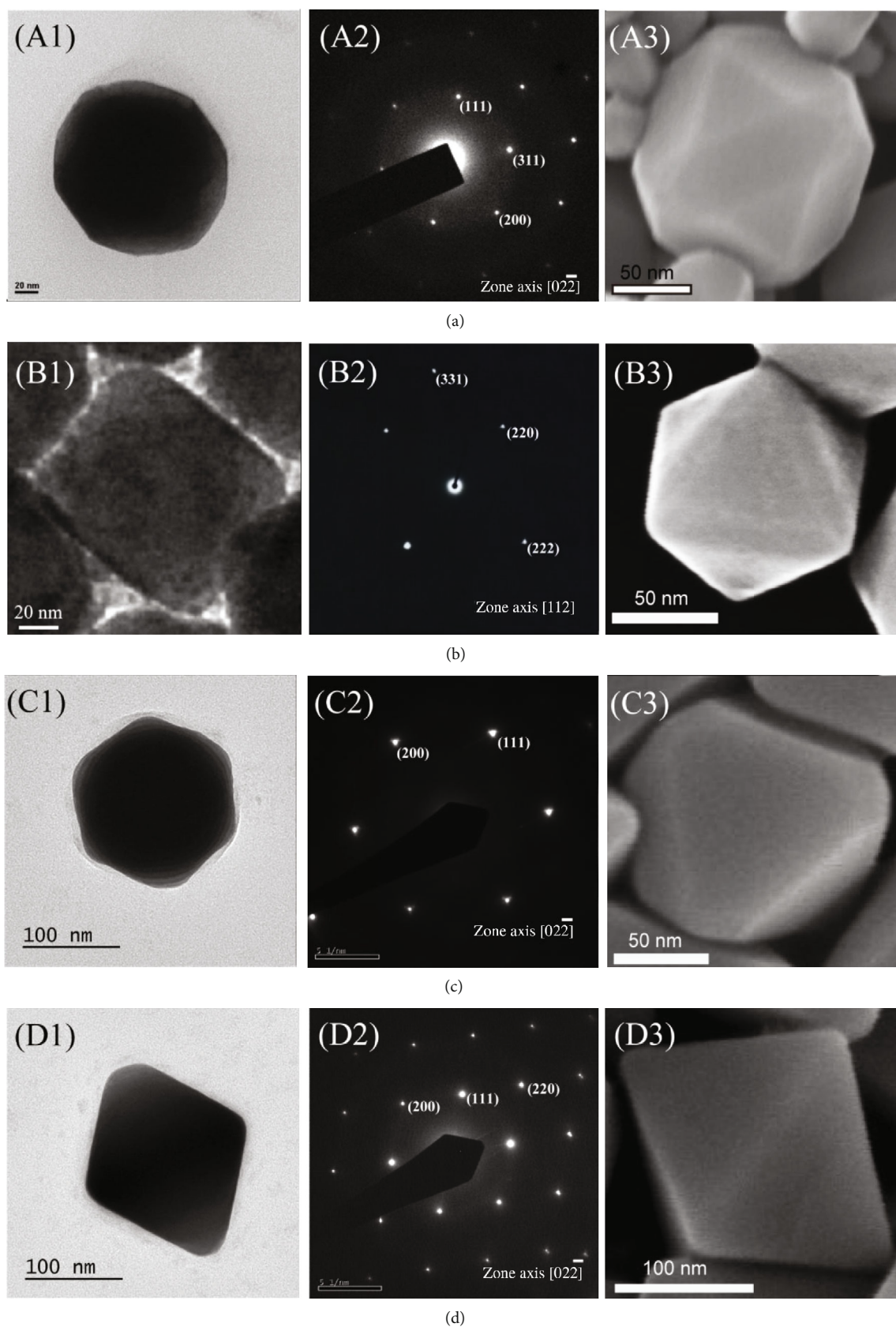Zone axis [0$\bar{2}$2]

5 1/nm

(D3)

100 nm

(d)

FIGURE 3: SEM images of the shape evolution of Cu nanoparticles with different reaction times: (a) 10 minutes, (b) 15 minutes, and (c) 20 minutes.
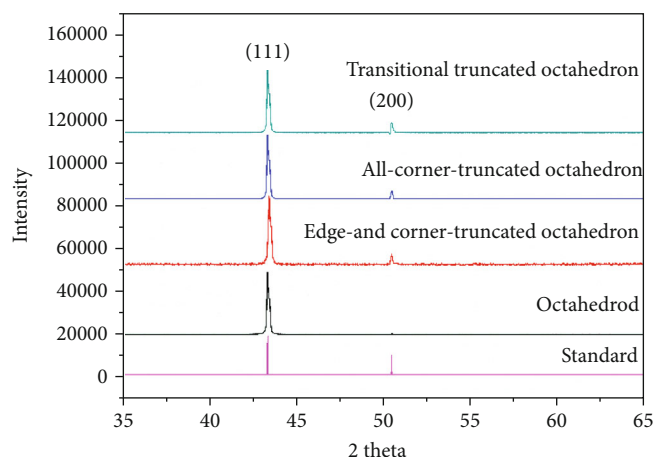
FIGURE 4: Powder X-ray diffraction patterns of different morphologies of Cu nanocrystals. A standard diffraction pattern of Cu is also given.
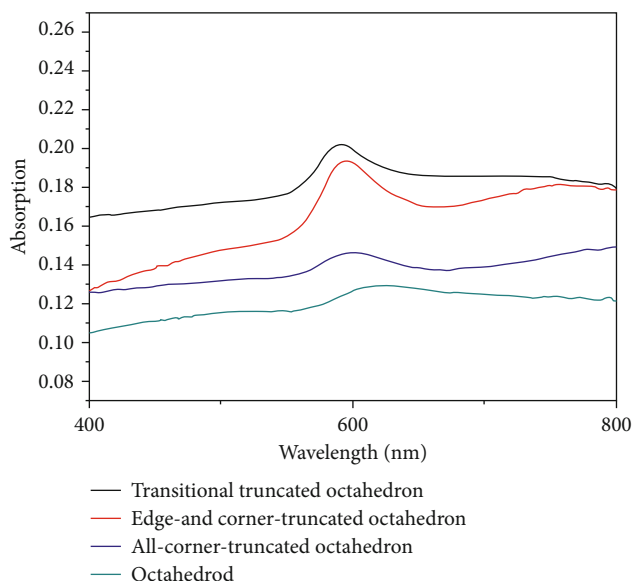

FIGURE 5: UV-visible spectra of Cu nanoparticles with the shape evolution from (a) a transitional truncated octahedron, (b) an edge- and corner-truncated octahedron, (c) an all-corner-truncated octahedron, and (d) an octahedron, which are located at 590 nm, 595 nm, 597 nm, and 620 nm, respectively.

relatively narrow peaks at 590 nm and 595 nm, respectively. Nevertheless, the all-corner-truncated octahedron and octahedron show broad bands at the location of 597 nm and 620 nm, respectively. This result indicates that the SPR band shifts red while the shape of nanoparticles evolves from a transitional truncated octahedral to octahedral, whose resonant bands are transferred from 590 nm to 620 nm.

The different reaction time greatly influences the morphology of the nanoparticles. The shape of nanoparticles changes from transitional truncated octahedra to edge- and corner-truncated octahedra, all-corner-truncated octahedra, and octahedra by increasing the reaction time in each batch.

According to the surface structure, a transitional truncated octahedron has a mix of {111}, {110}, and {100} facets exposed to the surfaces, and the {111} surface fraction increases continuously until the morphology evolves to octahedral whose surfaces are covered by {111} facets completely with increased reaction time. It reveals a fact that the formation of these Cu nanoparticles can be explained by the consequence of minimizing surface energy, which surface energies of different crystalline planes are in the sequence of $\gamma(110) > \gamma(100) > \gamma(111)$.

4. Conclusion

In conclusion, various single-crystalline Cu nanoparticles have been synthesized by tuning reaction time through a solution-based reduction reaction using TOP as a capping agent. The surface morphologies and projected images of nanoparticles have been characterized by SEM and TEM techniques. Four distinct morphologies have been observed. The UV-visible absorption spectra of these nanoparticles were also measured. The shape evolution of nanoparticles in the present synthetic system should be worthy of understanding the growth mechanism of Cu polyhedral structures, which can be a classic model for the fabrication of more various morphologies of Cu nanomaterials.

Data Availability

All the data used to support the findings of this study are included within the article.

Conflicts of Interest

The authors declare that they have no conflicts of interest.

Acknowledgments

Supplementary Materials

Other SEM images of copper nanocrystals with transitional truncated octahedral, edge-corner-transitional truncated octahedral, all-corner-truncated octahedral, and octahedral forms. *(Supplementary Materials)*

References

[1] Y. Xia, Y. Xiong, B. Lim, and S. E. Skrabalak, "Shape-Controlled Synthesis of Metal Nanocrystals: Simple Chemistry Meets Complex Physics?," *Angewandte Chemie, International Edition*, vol. 48, no. 1, pp. 60–103, 2009.

[2] A. R. Tao, S. Habas, and P. Yang, "Shape Control of Colloidal Metal Nanocrystals," *Small*, vol. 4, no. 3, pp. 310–325, 2008.

[3] S. M. Lee, S. N. Cho, and J. Cheon, "Anisotropic Shape Control of Colloidal Inorganic Nanocrystals," *Advanced Materials*, vol. 15, no. 5, pp. 441–444, 2003.

[4] X. Wang, J. Zhuang, Q. Peng, and Y. Li, "A general strategy for nanocrystal synthesis," *Nature*, vol. 437, no. 7055, pp. 121–124, 2005.

[5] F. Kim, S. Connor, H. Song, T. Kuykendall, and P. Yang, "Platonic Gold Nanocrystals," *Angewandte Chemie, International Edition*, vol. 116, no. 28, pp. 3759–3763, 2004.

[6] C. Li, K. L. Shuford, Q. H. Park et al., "High-Yield Synthesis of Single-Crystalline Gold Nano-octahedra," *Angewandte Chemie, International Edition*, vol. 46, no. 18, pp. 3264–3268, 2007.

[7] H. Song, F. Kim, S. Connor, G. A. Somorjai, and P. Yang, "Pt Nanocrystals: Shape Control and Langmuir–Blodgett Monolayer Formation," *The Journal of Physical Chemistry B*, vol. 109, no. 1, pp. 188–193, 2005.

[8] A. Sánchez-Iglesias, I. Pastoriza-Santos, J. Pérez-Juste, B. Rodríguez-González, F. J. García de Abajo, and L. M. Liz-Marzán, "Synthesis and Optical Properties of Gold Nanodecahedra with Size Control," *Advanced Materials*, vol. 18, no. 19, pp. 2529–2534, 2006.

[9] B. Lim, Y. Xiong, and Y. Xia, "A Water-Based Synthesis of Octahedral, Decahedral, and Icosahedral Pd Nanocrystals," *Angewandte Chemie, International Edition*, vol. 119, no. 48, pp. 9439–9442, 2007.

[10] K. Kwon, K. Y. Lee, Y. W. Lee et al., "Controlled Synthesis of Icosahedral Gold Nanoparticles and Their Surface-Enhanced Raman Scattering Property," *The Journal of Physical Chemistry C*, vol. 111, no. 3, pp. 1161–1165, 2006.

[11] D. Seo, J. C. Park, and H. Song, "Polyhedral Gold Nanocrystals withOhSymmetry: From Octahedra to Cubes," *Journal of the American Chemical Society*, vol. 128, no. 46, pp. 14863–14870, 2006.

[12] H.-J. Yang, S.-Y. He, H.-L. Chen, and H.-Y. Tuan, "Monodisperse Copper Nanocubes: Synthesis, Self-Assembly, and Large-Area Dense-Packed Films," *Chemistry of Materials*, vol. 26, no. 5, pp. 1785–1793, 2014.

[13] Y. Xiong, J. M. McLellan, J. Chen, Y. Yin, Z. Y. Li, and Y. Xia, "Kinetically Controlled Synthesis of Triangular and Hexagonal Nanoplates of Palladium and Their SPR/SERS Properties," *Journal of the American Chemical Society*, vol. 127, no. 48, pp. 17118–17127, 2005.

[14] S. Chen and D. L. Carroll, "Synthesis and Characterization of Truncated Triangular Silver Nanoplates," *Nano Letters*, vol. 2, no. 9, pp. 1003–1007, 2002.

[15] W. Niu, L. Zhang, and G. Xu, "Shape-Controlled Synthesis of Single-Crystalline Palladium Nanocrystals," *ACS Nano*, vol. 4, no. 4, pp. 1987–1996, 2010.

[16] C.-H. Kuo and M. H. Huang, "Facile Synthesis of Cu2O Nanocrystals with Systematic Shape Evolution from Cubic to Octahedral Structures," *Journal of Physical Chemistry C*, vol. 112, no. 47, pp. 18355–18360, 2008.

[17] G. H. Jeong, M. Kim, Y. W. Lee et al., "Polyhedral Au Nanocrystals Exclusively Bound by {110} Facets: The Rhombic Dodecahedron," *Journal of the American Chemical Society*, vol. 131, no. 5, pp. 1672-1673, 2009.

[18] W.-C. Huang, L.-M. Lyu, Y.-C. Yang, and M. H. Huang, "Synthesis of Cu2O Nanocrystals from Cubic to Rhombic Dodecahedral Structures and Their Comparative Photocatalytic Activity," *Journal of the American Chemical Society*, vol. 134, no. 2, pp. 1261–1267, 2011.

[19] Y. Xiong and Y. Xia, "Shape-Controlled Synthesis of Metal Nanostructures: The Case of Palladium," *Advanced Materials*, vol. 19, no. 20, pp. 3385–3391, 2007.

[20] I. Pastoriza-Santos, A. Sánchez-Iglesias, B. Rodríguez-González, and L. M. Liz-Marzán, "Aerobic Synthesis of Cu Nanoplates with Intense Plasmon Resonances," *Small*, vol. 5, no. 4, pp. 440–443, 2009.

[21] Y. Wang, A. V. Biradar, G. Wang et al., "Controlled Synthesis of Water-Dispersible Faceted Crystalline Copper Nanoparticles and Their Catalytic Properties," *Chemistry - A European Journal*, vol. 16, no. 35, pp. 10735–10743, 2010.

[22] T. Salmi and R. Hakkarainen, "Kinetic Study of the Low-Temperature Water-Gas Shift Reaction over a Cu—ZnO Catalyst," *Applied Catalysis*, vol. 49, no. 2, pp. 285–306, 1989.

[23] O. Jakdetchai and T. Nakajima, "Mechanism of the water-gas shift reaction over Cu(110), Cu(111) and Cu(100) surfaces: an AM1-d study," *Journal of Molecular Structure: THEOCHEM*, vol. 619, no. 1-3, pp. 51–58, 2002.

[24] T. Ressler, B. L. Kniep, I. Kasatkin, and R. Schlögl, "The Microstructure of Copper Zinc Oxide Catalysts: Bridging the Materials Gap," *Angewandte Chemie, International Edition*, vol. 44, no. 30, pp. 4704–4707, 2005.

[25] S. Vukojević, O. Trapp, J.-D. Grunwaldt, C. Kiener, and F. Schüth, "Quasi-Homogeneous Methanol Synthesis Over Highly Active Copper Nanoparticles," *Angewandte Chemie, International Edition*, vol. 44, no. 48, pp. 7978–7981, 2005.

[26] J. Tanori and M. P. Pileni, "Control of the Shape of Copper Metallic Particles by Using a Colloidal System as Template," *Langmuir*, vol. 13, no. 4, pp. 639–646, 1997.

[27] W.-Y. Ko, W.-H. Chen, S.-D. Tzeng, S. Gwo, and K.-J. Lin, "Synthesis of Pyramidal Copper Nanoparticles on Gold Substrate," *Chemistry of Materials*, vol. 18, no. 26, pp. 6097–6099, 2006.

[28] D. Mott, J. Galkowski, L. Wang, J. Luo, and C.-J. Zhong, "Synthesis of Size-Controlled and Shaped Copper Nanoparticles," *Langmuir*, vol. 23, no. 10, pp. 5740–5745, 2007.

[29] H. Guo, Y. Chen, M. B. Cortie et al., "Shape-Selective Formation of Monodisperse Copper Nanospheres and Nanocubes via Disproportionation Reaction Route and Their Optical Properties," *Journal of Physical Chemistry C*, vol. 118, no. 18, pp. 9801–9808, 2014.

[30] H. Guo, Y. Chen, H. Ping, J. Jin, and D.-L. Peng, "Facile synthesis of Cu and Cu@Cu–Ni nanocubes and nanowires in hydrophobic solution in the presence of nickel and chloride ions," *Nanoscale*, vol. 5, no. 6, pp. 2394–2402, 2013.

[31] S.-C. Lu, M.-C. Hsiao, M. Yorulmaz et al., "Single-Crystalline Copper Nano-Octahedra," *Chemistry of Materials*, vol. 27, no. 24, pp. 8185–8188, 2015.

[32] Z. Lyu, M. Xie, K. D. Gilroy et al., "A Rationally Designed Route to the One-Pot Synthesis of Right Bipyramidal Nanocrystals of Copper," *Chemistry of Materials*, vol. 30, no. 18, pp. 6469–6477, 2018.

[33] M. Luo, A. Ruditskiy, H. C. Peng et al., "Penta-Twinned Copper Nanorods: Facile Synthesis via Seed-Mediated Growth and Their Tunable Plasmonic Properties," *Advanced Functional Materials*, vol. 26, no. 8, pp. 1209–1216, 2016.

[34] P. Iyengar, J. Huang, G. L. De Gregorio, C. Gadiyar, and R. Buonsanti, "Size dependent selectivity of Cu nano-octahedra catalysts for the electrochemical reduction of CO2 to CH4," *Chemical Communications*, vol. 55, no. 60, pp. 8796–8799, 2019.

[35] A. S. Preston, R. A. Hughes, T. B. Demille, V. M. Rey Davila, and S. Neretina, "Dewetted nanostructures of gold, silver, copper, and palladium with enhanced faceting," *Acta Materialia*, vol. 165, pp. 15–25, 2019.

[36] K. L. Kelly, E. Coronado, L. L. Zhao, and G. C. Schatz, "The Optical Properties of Metal Nanoparticles: The Influence of Size, Shape, and Dielectric Environment," *The Journal of Physical Chemistry. B*, vol. 107, no. 3, pp. 668–677, 2003.